

Folding and Unfolding of an Elastinlike Oligopeptide: “Inverse Temperature Transition,” Reentrance, and Hydrogen-Bond Dynamics

Eduard Schreiner,¹ Chiara Nicolini,² Björn Ludolph,³ Revanur Ravindra,² Nikolaj Otte,¹ Axel Kohlmeyer,¹ Roger Rousseau,¹ Roland Winter,² and Dominik Marx¹

¹*Lehrstuhl für Theoretische Chemie, Ruhr-Universität Bochum, 44780 Bochum, Germany*

²*Physikalische Chemie I, Universität Dortmund, Otto-Hahn Strasse 6, 44227 Dortmund, Germany*

³*Max-Planck-Institut für Molekulare Physiologie, Otto-Hahn Strasse 11, 44227 Dortmund, Germany*

(Received 2 May 2003; published 7 April 2004)

The temperature-dependent behavior of a solvated oligopeptide, GVG(VPGVG), is investigated. Spectroscopic measurements, thermodynamic measurements, and molecular dynamics simulations find that this elastinlike octapeptide behaves as a two-state system that undergoes an “inverse temperature” folding transition and reentrant unfolding close to the boiling point of water. A molecular picture of these processes is presented, emphasizing changes in the dynamics of hydrogen bonding at the protein/water interface and peptide backbone librational entropy.

DOI: 10.1103/PhysRevLett.92.148101

PACS numbers: 87.15.He, 36.20.Ey, 82.20.Wt, 87.15.Aa

Elastin, a principal protein component in a vertebrate’s connective tissues, features very unusual viscoelastic properties [1–3]. Remarkably, upon *increasing* the temperature beyond 40 °C that protein *folds*, while normal proteins would undergo denaturation. The term “inverse temperature transition” (ITT) was coined for this apparently paradoxical change from a “disordered” (extended) to an “ordered” (folded) conformation upon heating. The origin of elastin’s properties is controversially discussed, calling on a wide array of concepts [1–6]. Beyond doubt is the decisive role of water as a plasticizer, dry elastin is *brittle* [3], but the aspect of the protein’s hydration water *dynamics* [7] remains unexplored.

Even its precursor, tropoelastin, is a complex compound, and its secondary structure still defeats elucidation. However, there is consensus that the repeat unit “VPGVG” [amino acids V (valine), P (proline), and G (glycine)] is crucial to elastins’ functionality. It was demonstrated [8] that GVG(VPGVG)_n display the ITT even in the limit $n = 1$. We therefore launched a joint experimental/simulation study of the octamer GVG(VPGVG) (≈ 640 Da). This model was chosen to allow for extensive molecular dynamics (MD) simulations with a thorough conformational sampling. To yield complementary experimental information circular dichroism (CD), Fourier-transform infrared (FT-IR), heat capacity, and thermal expansion coefficient measurements were carried out.

Solid-phase peptide synthesis using Fmoc protecting group strategies and chlorotriptyl linker was employed to obtain GVG(VPGVG) in sufficient quantity and purity. Based on phosphate buffered solutions at pH 7 with a peptide concentration of 0.5–1.0 mg/ml CD spectra were obtained from 2 to 95 °C (275–368 K) on a JASCO J-715 spectropolarimeter. The CD data are expressed as the mean residual ellipticity [θ] in ° cm² dmol⁻¹ from 190

to 260 nm. Secondary structure elements were determined using the convex constraint analysis (CCA) [9]. For the FT-IR spectra, the peptide was dissolved at a concentration of 5 wt.% in D₂O buffered at pD 7. A Nicolet MAGNA 550 spectrometer with a liquid nitrogen cooled MCT (HgCdTe) detector was used. The Fourier self-deconvolution was performed with a resolution enhancement factor of 1.8 and a bandwidth of 15 cm⁻¹. The fractional intensities of the secondary structure elements were calculated from a band fitting procedure using Gaussian-Lorentzian line shape functions [10]. Heat capacities C_p and thermal expansion coefficients α were obtained up to 120 °C (393 K) from differential scanning and pressure perturbation calorimetric (PPC) measurements, respectively, carried out on a VP calorimeter from MicroCal equipped with PPC accessory [11]. Sample concentration was 0.5–1.0 wt.% peptide in a 10 mM phosphate buffer.

The CD spectrum at 275 K features a pronounced negative band at 197 nm and a weaker one at 220 nm. Upon heating, the two minima shift such that an isodichroic point [8,12] occurs at ~ 212 nm; see Fig. 1(a). The developing intensity in the 206–212 nm region is characteristic for type II β turns [9], whereas the band around 197 nm is known from random or disordered structures [8,12]. A CCA decomposition [9] confirms that an equilibrium of two conformations fits the data best [8]. At the expense of the disordered structures, the weight of the β loop/strand structures increases from zero to about 40% upon increasing the temperature from 275 to 368 K. Although the analysis of the molar ellipticities at 212 and 220 nm yields a “formal” transition temperature of about 303–313 K, the ITT is very sluggish and broad.

At 275 K, the FT-IR spectrum in the amide I’ region 1575–1700 cm⁻¹ [see Fig. 1(b)] exhibits a maximum at 1641 cm⁻¹ due to a high content of disorder. Its

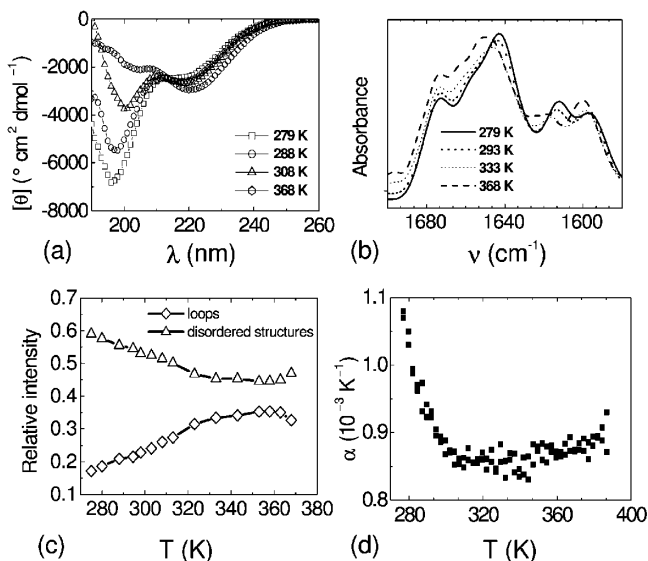


FIG. 1. (a) CD spectra; (b) Deconvoluted FT-IR absorption spectra; (c) Relative intensities of secondary structure elements obtained from the FT-IR analysis; (d) Thermal expansion coefficient.

intensity decreases upon heating and shifts to higher wave numbers, whereas a broad band, characteristic for loops, appears at $\sim 1650 \text{ cm}^{-1}$. The spectra were fitted based on various secondary structure elements (extended β chains, β sheets, disordered structures, α helices/loops, and β/γ turns). As with the CD analysis, an increase of loop structures is found up to 328 K at the expense of disordered conformations; see Fig. 1(c). According to FT-IR, the trend of peptide folding upon heating comes to a halt in the range of 333–353 K and even *reverses* at $T \geq 353 \text{ K}$ [see Fig. 1(c)], akin to what is observed in 1(b) around 1617 and 1595 cm^{-1} , which is tentatively assigned to different conformations of the terminal $-\text{COO}^-$ group. Thus, the ITT is succeeded by an unfolding or denaturation transition at higher temperatures.

To gain microscopic insights, MD was used to simulate the temperature behavior of the elastin model. We employ the all-atom CHARMM force field [13] and the TIP3P potential [14] for about 2100 water molecules in a 50 Å diameter spherical droplet subject to stochastic boundary conditions and a weak Berendsen thermostat as implemented in the EGO molecular dynamics package [15]. GVG(VPGVG) was capped by the methyl amine ($-\text{NH}-\text{CH}_3$) and acetyl ($-\text{CO}-\text{CH}_3$) group at its C- and N-terminus, respectively. Equilibration times from 2–5 ns were used prior to obtaining 32 ns trajectories at ten temperatures between 280–370 K.

To disentangle relevant folding modes from small-amplitude motion, we applied principal component analysis [16]. By diagonalizing the covariance matrix, $\mathbf{M} = \langle [\mathbf{x}(t) - \langle \mathbf{x} \rangle] \cdot [\mathbf{x}(t) - \langle \mathbf{x} \rangle]^T \rangle$, its $3N - 6$ normalized eigenvectors $\{\mathbf{m}_i\}$ with nonzero eigenvalues $\{\lambda_i\}$ provide a basis in which the peptide motion may be decomposed;

only backbone heavy atoms were included, and each side chain accounted for by a united atom yielding $N = 38$. Upon projecting the MD trajectories onto the eigenvectors, $\tilde{\mathbf{m}}_i = [\mathbf{x}(t) - \langle \mathbf{x} \rangle] \cdot \mathbf{m}_i$, it is found that the eigenvector associated with the largest eigenvalue λ_1 describes the opening and closing motion of the peptide and is present at *all temperatures*. At low temperatures, this projection possesses a bimodal distribution function, $P(\tilde{\mathbf{m}}_1)$, which adopts a broad and skewed shape upon heating. Since the higher-order modes have fairly symmetric, unimodal, and narrow distributions that do not change much with temperature, we can use $\tilde{\mathbf{m}}_1$ as a reaction coordinate or order parameter yielding an effective free energy profile $\Delta F = -k_B T \ln[P(\tilde{\mathbf{m}}_1)/P(\tilde{\mathbf{m}}_1^{\text{ref}})]$; see Fig. 2. At low temperatures, there is a global minimum ($\tilde{\mathbf{m}}_1 \approx +5 \text{ \AA}$ at 280 K) and a local minimum ($\tilde{\mathbf{m}}_1 \approx -20 \text{ \AA}$) that can be associated with extended and folded conformations, respectively; see insets of Fig. 2. At about 330 K, ΔF adopts a very flat single-minimum shape, and the relative weight of the folded state is maximum. Above 330 K, the local minimum of the folded state is less discernible, and the peptide *stretches*. This is consistent with FT-IR data in that folding initially increases upon raising the temperature, but is followed by a trend reversal.

Confirmation of *unfolding* behavior comes from both C_p and α ; see Fig. 1(d). In PPC the thermal expansion coefficient of the partial volume of the peptide is measured including its intrinsic volume as well as volume changes due to interactions with the solvent relative to pure buffer. At low temperatures α is large, which is consistent with a significantly hydrated extended structure. Thermal activation leads to a release of this water from the surface. Once released, it no longer contributes to the partial volume of the peptide

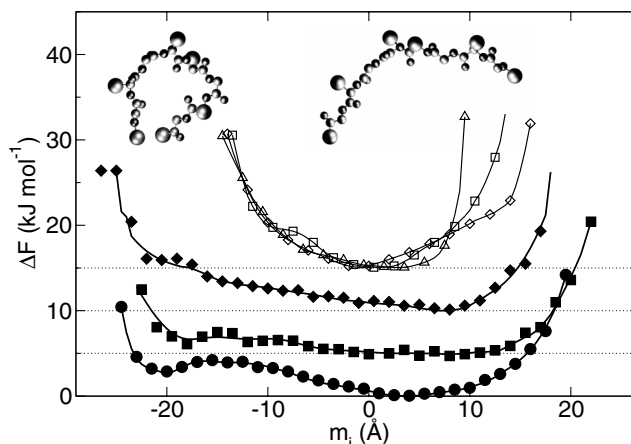


FIG. 2. Free energy profile along the order parameter coordinate $\tilde{\mathbf{m}}_1$ at 280 K (●), 330 K (■), and 370 K (◆). For comparison, $\Delta F(\tilde{\mathbf{m}}_i)$ is shown at 370 K for $\tilde{\mathbf{m}}_2$ (◇), $\tilde{\mathbf{m}}_3$ (□), and $\tilde{\mathbf{m}}_4$ (△) in the topmost panel. Insets: snapshots of representative folded (left: $R_{\text{CN}} \approx 5 \text{ \AA}$) and extended (right: $R_{\text{CN}} \approx 22 \text{ \AA}$) conformations.

and hence to α . This is followed by a plateau region of low α from about 303–313 K to 353–363 K, where α increases again. The smallest α is found in an intermediate regime that corresponds to the more compact folded loop state. The increase in α at high temperature can be interpreted in terms of a more pronounced hydration upon peptide unfolding. Similarly, C_p that is ≈ -0.43 kJ/mol K at 275 K increases initially and reaches a maximum of ≈ -0.33 kJ/mol K around 343 K, until it comes back at 393 K to its initial low-temperature value (not shown). Thus, thermodynamic quantities suggest that at unusually high temperatures the peptide changes back to a state that is similar to the low-temperature one and underscores the importance of the peptide/water interface.

Our MD results indicate a distinct difference in the hydrogen-bond (HB) arrangements between extended and folded forms. The latter is characterized by 3–6 peptide-peptide HBs and 1–3 water-bridged peptide-peptide contacts; both features do not occur in extended structures. Upon closing the number of water molecules within the first solvation shell of the backbone decreases by $\approx 20\%$, and the temperature dependence of the average number of peptide-peptide HBs and bridging water molecules (not shown) increases up to 330 K and subsequently decreases. There is no such correlation to be found for the water molecules about the hydrophobic side chains: their number is insensitive to the peptide conformation and decays monotonously with temperature. This suggests that a hydrophobic collapse as induced by solvation changes of hydrophobic side chains is not operative in this small peptide.

We therefore consider the intermittent HB autocorrelation function [17–19], $c(t) = \langle h(0)h(t) \rangle / \langle h \rangle$, i.e., the probability that a HB, which was intact at $t = 0$, is intact at time t ; $h(t) = 1$ if a particular HB exists at time t . The function [18,19] $n(t) = \langle h(0)[1 - h(t)]H(t) \rangle / \langle h \rangle$ is the conditional probability that a HB, which was intact at $t = 0$, is broken at time t given that the donor/acceptor partners are still close enough to potentially form a HB. Following [18], we formulate a rate equation for the “reactive flux” beyond the transient period, $-\dot{c}(t) = kc(t) - \tilde{k}n(t)$, where k and \tilde{k} are the rate constants for HB breaking and reformation, respectively. This analysis was performed for various HB classes: between water molecules in the bulk c_{bb} , the peptide and first shell solvation water c_{ps} , direct HB contacts of the peptide with itself c_{pp} , between two water molecules both located in the first solvation shell of peptide side chains c_{sc} , and water-mediated peptide-peptide bridges c_{psp} .

For bulk water, see Fig. 3, both time constants k_{bb} and \tilde{k}_{bb} show a simple Arrhenius behavior, $k_x = A_x \exp[-E_x^\ddagger/k_B T]$, at all temperatures (with $E_{bb}^\ddagger \approx 8$ –9 kJ/mol and $\tilde{E}_{bb}^\ddagger \approx 5$ –6 kJ/mol). Both HB breaking and reforming increase *constantly* with temperature in the bulk. The same is true for the breaking of HBs

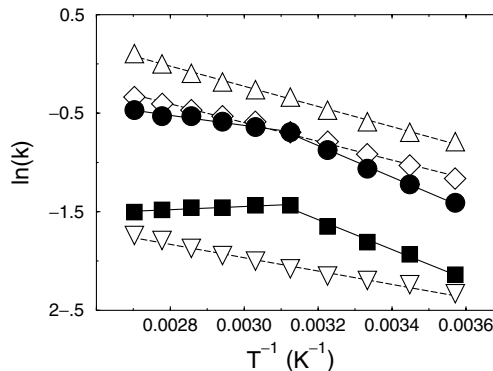


FIG. 3. Arrhenius plot of rate constants for HB breaking k_{ps} (●), k_{bb} (△), k_{sc} (◇) and HB reformation \tilde{k}_{ps} (■), \tilde{k}_{bb} (▽); note that akin to $\ln(k_{sc})$, $\ln(\tilde{k}_{sc})$ vs $1/T$ is linear in the entire temperature range with a slope similar to $\ln(\tilde{k}_{bb})$, and thus it is not shown. The symbol sizes cover the error bars, and the lines are linear fits including all temperatures (dashed lines) or separately the regimes above and below 330 K (solid lines).

between water molecules solvating side chains where $E_{sc}^\ddagger \approx 9$ kJ/mol as in the bulk. Thus, there is no indication of changes of the solvation shell about the side chains. This is different for the peptide-water HBs where *two distinct Arrhenius regimes* are observed. Below 320 K the activation energy $E_{ps}^\ddagger \approx 13$ kJ/mol to break an interfacial HB is higher than that in the bulk, whereas above 330 K it is much lower (≈ 4 kJ/mol). Likewise, HB reforming at the interface, up to 320 K, $\tilde{E}_{ps}^\ddagger \approx 11$ kJ/mol but at 330 K the apparent activation energy essentially vanishes. Thus, the temperature dependence of the dynamics of peptide-water HBs is in qualitative accord with the thermodynamic data, which also indicate an overall decrease in their “strength.” Note that the small size of the peptide does not allow for well-defined “phase transitions.” Hence, only two temperature regimes are apparent: “folding” at $T < 330$ K and “unfolding” at $T > 330$ K with only a narrow temperature range around $T \approx 330$ K where one observes the maximally folded state.

This change in HB kinetics is correlated with a maximized number of peptide-peptide HBs at 330 K. They exhibit an activation barrier for breaking, $E_{pp}^\ddagger \approx 8$ kJ/mol above 320 K, which is *twice* that for peptide-water HBs in this regime, and thus stabilize the folded state. In contrast, the number of peptide-water HBs *decreases* from 280 to 370 K (not shown). Thus, at low temperatures, peptide-water interfacial HBs seem to stabilize the open/extended state relative to the folded one. The increase of thermal energy decreases the stability of the open state but has less effect on the folded state, which is in part stabilized by peptide-peptide HBs.

The link between HBs and peptide motion is established by examining the dynamics of the reaction

coordinate \tilde{m}_1 as described by $c_m(t) = \langle \tilde{m}_1(0)\tilde{m}_1(t) \rangle / \langle \tilde{m}_1(0)\tilde{m}_1(0) \rangle$ and its relaxation time τ_m . For temperatures in which ΔF shows two minima (see Fig. 2), $\tau_m \approx 300$ ps is roughly constant. In the range 330–370 K there is a progressive speed increase ($\tau_m \approx 140$ ps at 370 K) that reflects the steepening of the free energy surface in the folded regime, $\tilde{m}_1 \ll 0$. These findings correlate well with large peptide backbone fluctuations observed by NMR for water swollen elastins [20] and are consistent with the mean effective correlation time ≈ 500 ps for poly(GVPGV) at 298 K obtained from ^{13}C NMR relaxation [21]. Most remarkably, the dynamics of the peptide mirrors that of the interfacial HBs despite the 2 orders of magnitude difference in time scale.

Despite the increase in peptide-peptide HBs, there is an overall increase of freedom in the motion of the peptide backbone as evidenced by the short lifetime of both intramolecular and bridging HB contacts (τ_{pp} and $\tau_{psp} \leq 1$ –2 ps). This is also reflected in its total entropy change estimated from a quasiharmonic approximation [16] which is positive and increasing by ≈ 0.3 kJ/mol K from 280 to 370 K. This is consistent with the experimental entropy increase of 0.11 and 0.15 kJ/mol K (298 K) obtained from van't Hoff analysis [8] of the CD and FT-IR data, respectively. The entropy increase of the backbone upon folding is similar in spirit to various librational entropy models [1,2]. Thus, the opening and closing motion of the peptide itself has a *stabilizing* entropic contribution to the observed *folding* behavior. This is also in accord with the C_p maximum observed in this temperature regime, recalling that C_p is proportional to the entropy fluctuations $\langle (\delta S)^2 \rangle$. Ultimately, increasing backbone fluctuations above 330 K will result in rapid breaking of peptide-peptide bonds and thus counteracts the stabilization of the folded state, eventually leading to unfolding at higher temperature.

In conclusion, we find a two-state folding/unfolding scenario, as inferred from both experiment and simulation, which is traced back to changes in the hydrogen bonding at the peptide/water interface. The proposed mechanism has a striking resemblance to the recently advocated segregation mechanism in methanol/water mixtures [22]. According to this picture, the *polar interactions of water with hydrophilic groups*, i.e., hydrogen-bonding, exerts a stronger influence than water restructuring induced by hydrophobic groups. Finally, the proposed mechanism might lead to novel concepts for rational molecular design of biopolymeric materials for thermomechanical devices [1].

We thank A. Chandra, A. Geiger, H. Grubmüller, M. Müller, H. Weingärtner, and X.-Y. Yu for discussions as well as DFG (FOR 436) and FCI for support.

-
- [1] D.W. Urry, *Angew. Chem., Int. Ed. Engl.* **32**, 819 (1993); *J. Phys. Chem. B* **101**, 11007 (1997).
 - [2] L. Debelle and A. M. Tamburro, *Int. J. Biochem. Cell Biol.* **31**, 261 (1999).
 - [3] L. Debelle and A. J. P. Alix, *Biochimie* **81**, 981 (1999).
 - [4] C. A. J. Hoeve and P. J. Flory, *Biopolymers* **13**, 677 (1974).
 - [5] Z. R. Wasserman and F. R. Salemme, *Biopolymers* **29**, 1613 (1990).
 - [6] B. Li, D. O. V. Alonso, and V. Daggett, *J. Mol. Biol.* **305**, 581 (2001); B. Li, D. O. V. Alonso, B. J. Bennion, and V. Daggett, *J. Am. Chem. Soc.* **123**, 11991 (2001).
 - [7] M. Tarek and D. J. Tobias, *Phys. Rev. Lett.* **89**, 275501 (2002); *Phys. Rev. Lett.* **88**, 138101 (2002); *J. Am. Chem. Soc.* **121**, 9740 (1999).
 - [8] H. Reiersen, A. R. Clarke, and A. R. Rees, *J. Mol. Biol.* **283**, 255 (1998).
 - [9] A. Perczel, M. Hollósi, G. Tusnády, and G. D. Fasman, *Protein Eng.* **4**, 669 (1991).
 - [10] G. Panick *et al.*, *J. Mol. Biol.* **275**, 389 (1998).
 - [11] R. Ravindra and R. Winter, *Chem. Phys. Chem.* **4**, 359 (2003).
 - [12] D.W. Urry, R. G. Shaw, and K. U. Prasad, *Biochem. Biophys. Res. Commun.* **130**, 50 (1985).
 - [13] A. D. MacKerell, Jr. *et al.*, *J. Phys. Chem. B* **102**, 3586 (1998).
 - [14] W. L. Jorgensen *et al.*, *J. Chem. Phys.* **79**, 926 (1983).
 - [15] M. Eichinger, H. Heller, and H. Grubmüller, in *Molecular Dynamics on Parallel Computers*, edited by R. Esser, P. Grassberger, J. Grotendorst, and M. Lewerenz (World Scientific, Singapore, 2000).
 - [16] A. E. Garcia, *Phys. Rev. Lett.* **68**, 2696 (1992); A. Amadei, A. B. M. Linssen, and H. J. C. Berendsen, *Proteins Struct. Funct. Genet.* **17**, 412 (1993); I. Andricioaei and M. Karplus, *J. Chem. Phys.* **115**, 6289 (2001); A. L. Tournier and J. C. Smith, *Phys. Rev. Lett.* **91**, 208106 (2003).
 - [17] F. H. Stillinger, *Adv. Chem. Phys.* **31**, 1 (1975).
 - [18] A. Luzar and D. Chandler, *Phys. Rev. Lett.* **76**, 928 (1996); A. Luzar and D. Chandler, *Nature (London)* **379**, 55 (1996).
 - [19] A. Chandra, *Phys. Rev. Lett.* **85**, 768 (2000).
 - [20] A. Perry, M. P. Stypa, J. A. Foster, and K. K. Kumashiro, *J. Am. Chem. Soc.* **124**, 6832 (2002).
 - [21] D. Kurková *et al.*, *Biomacromolecules* **4**, 589 (2003).
 - [22] S. Dixit *et al.*, *Nature (London)* **416**, 829 (2002).